American Journal of Nanosciences
2017; 3(4): 81-85
http://www.sciencepublishinggroup.com/j/ajn
doi: 10.11648/j.ajn.20170304.12
ISSN: 2575-484X (Print); ISSN: 2575-4858 (Online)

Synthesis, Characterization, Effect of Temperature on Band Gap Energy of Molybdenum Oxide Nano Rods and Their Antibacterial Activity

Azad Kumar*, Gajanan Pandey

Department of Applied Chemistry, School for Physical Sciences, Babasaheb Bhimrao Ambedkar University, Lucknow, India

Email address:
Kumarazad20@gmail.com (A. Kumar)
*Corresponding author

To cite this article:
Azad Kumar, Gajanan Pandey. Synthesis, Characterization, Effect of Temperature on Band Gap Energy of Molybdenum Oxide Nano Rods and Their Antibacterial Activity. *American Journal of Nanosciences.* Vol. 3, No. 4, 2017, pp. 81-85. doi: 10.11648/j.ajn.20170304.12

Received: July 26, 2017; **Accepted**: August 16, 2017; **Published**: December 18, 2017

Abstract: In this study, the nano rods of molybdenum oxide were prepared by the thermo chemical method. The prepared molybdenum oxide nano rods were characterized by UV-Visible spectrophotometer, band gap energy, FT-IR spectrophotometer, XRD, SEM, and TEM techniques. The prepared molybdenum oxide nano rods were used for anti bacterial activity. The XRD analysis showed the formation of crystalline nano rods. The FT-IR and UV-Vis analysis give the peak at 1120 cm^{-1} and 246 nm which confirm the formation of nano rods. The SEM and TEM analysis also confirmed the formation of nano rods. The band gap energy of MoO_3 nano rods were observed 3.67, 3.54, 3.45 and 3.36 eV at 400, 500, 600 and 700°C temperatures. The MoO_3 nano rods gave the positive antibacterial activity against *S. Aureus* pathogens.

Keywords: Molybdenum Oxide, S. Aureus, Nano Rods, Band Gap Energy

1. Introduction

Molybdenum (VI) oxide (MoO_3) is a wide band gap semiconductor. It is n-type semiconductor which have distinctive electrochromic, thermochromic, and photochromic properties. It has been widely investigated as smart materials for catalysis [1-2], sensors lubricants, lithium battery, organic solar cells and display materials [3-4]. It is actually realized that purity of phase MoO_3 depended on the manufactured technique and experimental conditions [5-6]. Impressive advances have been accomplished recently for the size and phase controlled synthesis of MoO_3 with enhanced catalyst properties [7-9].

In spite of the fact that exploration on molybdenum oxide (MoOx) nano rods began moderately late, MoOx nano rods are currently indicating the potential for both major research and applications in industry [10-11]. MoOx nano rods speak to the appealing building block for dynamic nano devices, by controlling the development and association. They can be utilized to deliver various novel, profoundly effective, strong, incorporated nanoscale devices, including field emission devices (FED) and photo detector [12-13]. The nano rods of MoO_3 are typically cylindrical, hexagonal, square, or triangular in cross-section [14].

The utilization of molybdenum-based catalysts is in the hydride sulfurization (HDS) of petroleum oil, petrochemicals and coal-derived liquids [15-16]. The catalyst MoS_2 supported on alumina and advanced by cobalt or nickel and is prepared by sullfiding cobalt and molybdenum oxides on alumina [17]. As the world supply of unrefined petroleum is additionally expanded and low-sulfur crudes become less accessible, molybdenum-based catalyst will increase in use [18]. Molybdenum is not only allowed for economical and practical fuel refining as well as contributes to a more secure environment through lower sulfur emission [19]. Molybdenum Catalysts are resistant to poisoning by sulfur and, for instance, catalyze transformation of hydrogen and carbon monoxide from the pyrolysis of waste materials to alcohols in the presence of sulfur, under conditions that would harm valuable metal catalysts. Also, Mo-based catalysts have been used in the conversion of coal to hydrocarbon liquids [20-22].

2. Methods and Materials

2.1. Synthesis of MoO_3

MoO_3 was synthesized by thermal method. In this method, 10 mL 0.2 M of ammonium heptamolybdate tetrahydrate was take in the beaker and stirred for 10 min to obtain a clear solution. Then 5 mL of concentrated HNO_3 was added drop-wise to the above solution and stirred for 10 min. The mixture was heated to 100°C for 2 h. After 2 h of heating, the mixture was allowed to cool down to room temperature. The product was dried at 70°C in the oven for 12 h. This product was calcined at different temperature such as 400°C, 500°C, 600°C and 700°C for 4 h, in muffle furnace. After calcinations the product can be used for further study [23-24].

The prepared molybdenum oxide nano rods were characterized by UV-Visible spectrophotometer, FT-IR, UV-Visible spectrophotometer, XRD, SEM, EDS, and TEM techniques.

3. Results and Discussion

3.1. X-Ray Diffraction Analysis

The prepared molybdenum oxide nano rods were analyzed by XRD for the determination of phase and symmetry. Figure 1 shows XRD pattern for molybdenum oxide nanoparticles in which number of peaks are observed at 30^O angle which is due to the formation of high crystalline molybdenum oxide nano rods. The peaks were observed at 2θ 27.3, 58.5, 64.7 and 72.8. Sharp peaks were obtained corresponding to the planes(111), (201), (211) and (312) indicating the MoO_3 nano rods and which was found to be highly crystalline in nature [25-26].

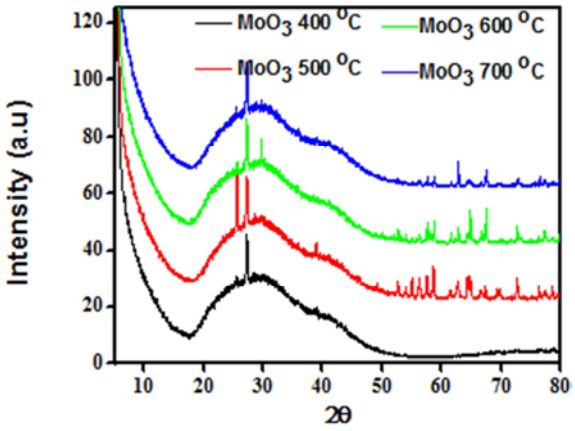

Figure 1. *XRD spectra of MoO_3 nanomaterials at different temperature.*

The planes (111), (201), (211) and (312) correspond to the mixed phase that contains molybdenum oxide nanoparticles and molybdenum oxide nanorods in the prepared samples of Molybdenum oxide. The effect of temperature was found on the synthesis of Molybdenum oxide nanorods, peak intensity increased with increasing of temperature, this is because that the crystalline nature of molybdenum oxide increase with increasing temperature of reaction. [27-28].

3.2. FTIR Spectra

The IR spectra shows distinct bands at 1120 cm^{-1}, 1622 $cm^{-1}$and 3453 cm^{-1}, which are due to the formation of MoO_3, presence of carbonyl impurity in the sample (Figure 2). The band observed at 3452 is due to the moisture absorbed from the atmospheric air during the storage. The spectrum also contains distinct peaks at 476 cm-1 and 804 cm^{-1} which

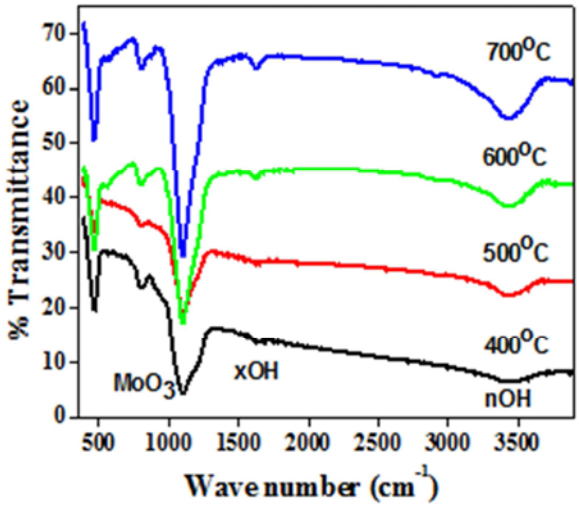

Figure 2. *FTIR spectra of Molybdenum oxide at different temperature.*

3.3. UV-Visible Spectra

The dependence of the UV-Visible absorption spectra of the molybdenum oxide nano rods are shown in Figure 3. The absorbance was seen across the visible range from 600 to 700nm. The Figure 3 shows the absorption band at 240 nm which confirms the formation of MoO_3 nanoparticles. The peak is observed at 240 nm, due to the d-d transition in the molybdenum oxide [29]. The wavelength increase with increasing the temperature of reaction, this is due to the transition shifted into red shift or higher wavelength. It means that the transition at high temperature occur at lower energy. The crystallinity is increase with increasing the wavelength of prepared samples of MoO_3 [30].

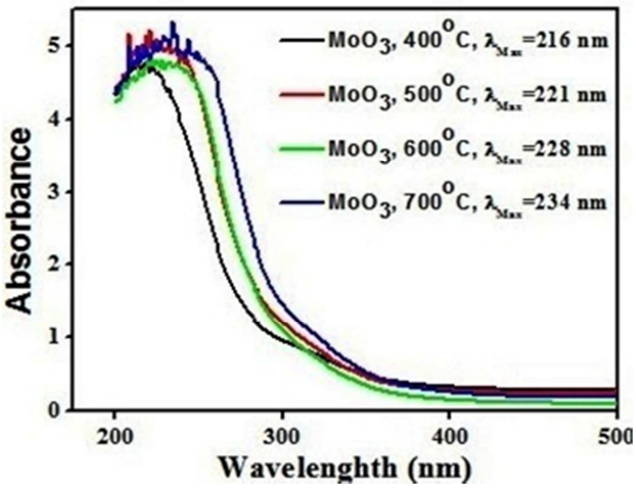

Figure 3. *UV Visible spectra of Molybdenum oxide at different temperature.*

3.4. Determination of Optical Band Gap of Nanocomposites

The band gap of Molybdenum oxide was determined from absorption spectra and Tauc relation (Eq. 2)

$$\alpha h\nu = B(h\nu - Egap)^{m} \quad (2)$$

where α is the absorption coefficient, hν is the photon energy, and m = 1/2 for direct band gap material shown in Figure4. To described a direct method for fitting and determination of band gap using Tauc relation [31-32]. Figure 4 yields an *Eg* value of MoO_3 nano rods at various temperatures. The band gap energy of MoO_3 is 3.67, 3.54, 3.45 and 3.36 eV at 400, 500, 600 and 700°C temperatures respectively. The band gap energy of MoO_3 nano rods are decrease with increase of temperature from 400°C to 700°C. The decrease in band gap energy is due to the formation of perfect crystal structure and increase the size of nano rods [33].

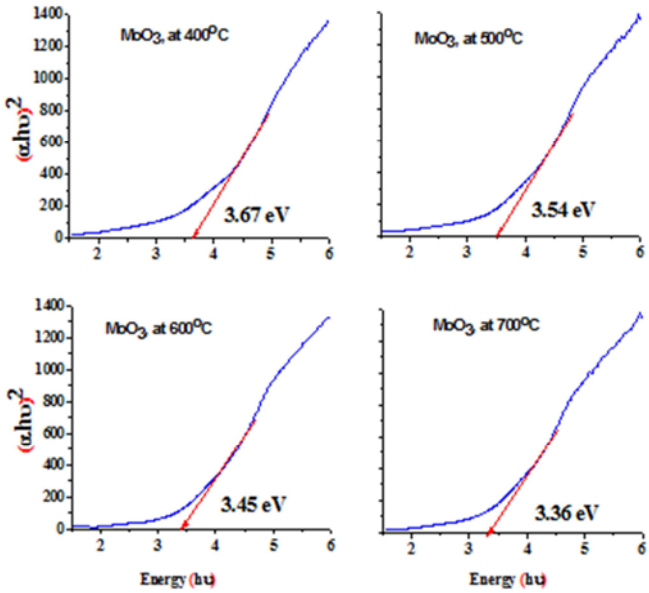

Figure 4. *Band gap energy of Molybdenum oxide at different temperature.*

3.5. Scanning Electron Microscopy (SEM)

SEM microstructure of the electrochemical reduction derived molybdenum oxide nano rod reveals the presence of dense agglomerations Figure 5 shows these nano rods having regular shape and their distribution is not uniform. This is probably due to the partial solubility of the surfactant in the solvent under the given experimental conditions. Figure 5 shows the presence of crystalline nano rods that are arranged irregularly [34].

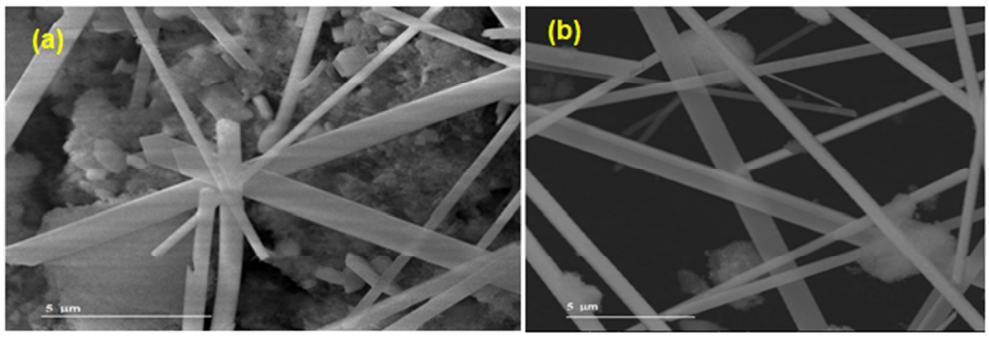

Figure 5. *SEM image of Molybdenum oxide at (a) 400°C and (b) 700°C.*

3.6. Transmission Electron Microscopy (TEM)

TEM microscopic study has been done for the determination of surface morphology of prepared molybdenum oxide nano rods as shown in Figure 6. TEM microstructure clearly indicated the formation of nano rods, which are micrometer range. The rods like structures are observed in the prepared sample of Molybdenum oxide which having the average particle size 0.5 to 1 µm range [35]. The effect of temperature was observed. The temperature of reaction was increased, the crystallinity of prepared samples of Molybdenum oxide nanorods increase. It is shown in Figure 6. The symmetry of a crystal can be directly observed through the strong dynamical diffraction effects using CBED [36]. Thus the CBED technique is a powerful tool to determine the space group of an unknown

phase. The CBED pattern is showing in Figure 7. The CBED pattern gives the information about the crystallinity of prepared sample. The MoO_3 was found in the perfectly crystalline in nature and in nanometric range. The Figure 7 showed the effect of temperature on the CBED pattern. The crystallinity of molybdenum oxide sample is increase with increase in the temperature of reaction (Figure 7a and 7b).

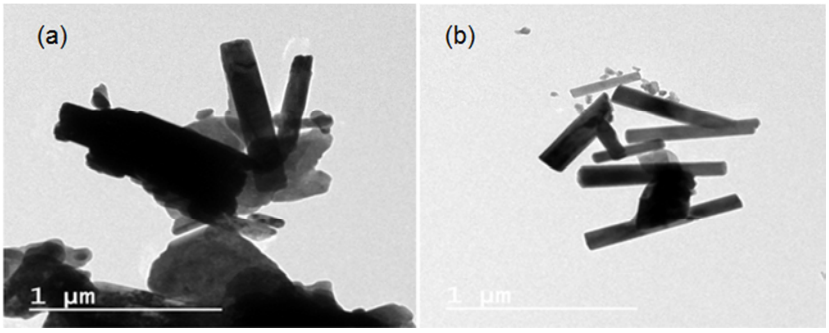

Figure 6. *TEM image of Molybdenum oxide at at (a) 400°C and (b) 700°C.*

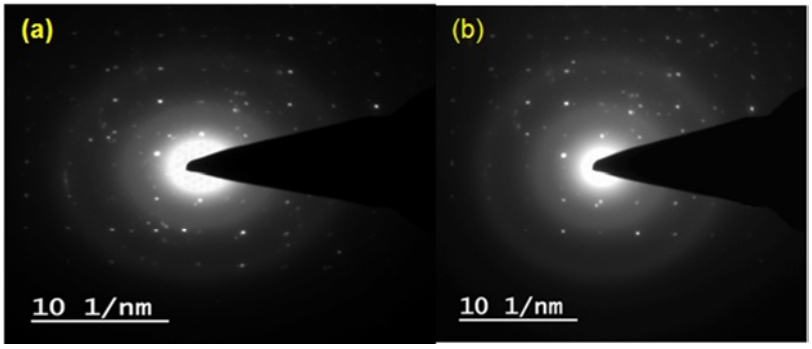

Figure 7. *TEM CBED pattern of Molybdenum oxide at at (a) 400°C and (b) 700°C.*

3.7. Antibacterial Activity

Analysis of Antibacterial activity of MoO_3 700(7), MoO_3 600(8) and MoO_3 500(9) samples which were in powder form. The solutions of these samples were prepared of 30 mg/ml concentration. With the help of Antibiotic Sensitivity Test or Agar Well Diffusion method, we were analyzed the Antibacterial activity of the samples. These were the E. coli MTCC 1687, P. Aeuginosa MTCC 741 and S. Aureus MTCC 902 pathogens using against antibacterial activity (Table 1). Only sample MoO_3 700(7), MoO_3 600(8) gave the result against S. Aureus pathogens and rest of samples does not give any result against all these three pathogens (shown in Table 1 and Figure 8). The prepared nano rods at different temperature are not capable to give antibacterial activity. The nano rods prepared at 600 and 700°C are showing the antibacterial activity. This is because that at higher temperature the perfectly crystalline nano rods were prepared and which is highly active against antibacterial activity [37-40].

Table 1. *Analysis of Antibacterial activity of MoO_3 700(7), MoO_3 600(8) and MoO_3 500(9).*

S.No.	Pathogen	Zone Of Inhibition (mm)		
		7	8	9
1.	*E. coli*	-	-	-
2.	*P.aeruginosa*	-	-	-
3.	*S. aureus*	15.0	17.5	-

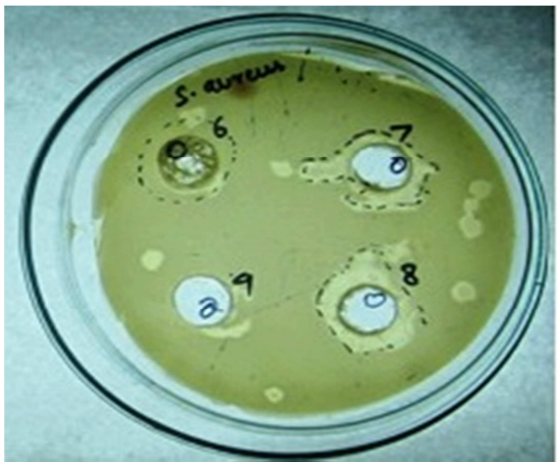

Figure 8. *Above figure represent the result of Analysis of Antibacterial activity of MoO_3 700(7), MoO_3 600(8) and MoO_3 500(9) against different pathogens (right to left; P. aeruginosa, S. aureus) in which clear zone of hydrolysis shown that marked in a circle.*

4. Conclusion

The nano rods of molybdenum oxide were prepared by the thermo chemical method. The XRD analysis showed the formation of crystalline nano rods. The FT-IR and UV-Vis analysis give the peak at 1120 cm^{-1} and 246 nm which confirm the formation of nano rods. The SEM and TEM analysis also confirmed the formation of nano rods which is

in 0.5-1 μm. The band gap energy of MoO_3 nano rods were observed 3.67, 3.54, 3.45 and 3.36 eV at 400, 500, 600 and 700°C temperatures. The effect of temperature on band gap energy was observed. It was found that with increases in the temperature, the band gap energy decreased. The MoO_3 nano rods gave the positive antibacterial activity against *S. Aureus* pathogens.

Acknowledgements

We thanks for financial assistance to UGC, Government of India is acknowledged. The authors also acknowledge the support provided by the Babasaheb Bhimrao Ambedkar University, Lucknow, India

References

[1] Y. Shi, B. Guo, S. A. Corr, Q. Shi, Y. S. Hu, K. R. Heier, L. Chen, R. Seshadri, G. D. Stucky, NanoLett. 9, 4215–4220 (2009).

[2] D. P. Debecker, M. Stoyanova, U. Rodemerck, E. M. Gaigneaux, Stud. Surf. Sci. Catal. 175, 581–585 (2010).

[3] Y. Chen, C. Lu, L. Xu, Y. Ma, W. Hou, J. Zhu, Cryst. Eng. Comm. 12, 3740-3747 (2010).

[4] C. Raj, A. C. Bose, Beilstein J. Nanotechnol. 2, 585–592(2011).

[5] S. Ganguly, R. George, Bull. Mater. Sci. 30, 183–185(2007).

[6] W. Dong, H. Huang, Y. Zhu, X. Li, X. Wang, C. Li, B. Chen, G. Wang, Z. Shi, Nanotechnology 23, 425602 (2012).

[7] L. Zhou, L. Yang, P. Yuan, J. Zou, Y. Wu, C. Yu, J. Phys. Chem. C 114, 21868-21872 (2010).

[8] A. M. Hashema, H. Groult, A. Mauger, K. Zaghib, C. M. Julien, J. Power Sources 219 126-132(2012).

[9] Q. Xia, H. Zhao, Z. Du, J. Wang, T. Zhang, J. Wang, P. J. Power Sources 226, 107-111 (2013).

[10] F. J. Zhang, D. W. Zhao, Z. L. Zhuo, H. Wang, Z. Xu, Y. S. Wang, Sol. Energy Mater. Sol. Cells 94, 2416-2421 (2010).

[11] F. Cheng, G. Fang, X. Fan, N. Liu, N. Sun, P. Qin, Q. Zheng, J. Wan, X. Zhao, Sol. Energy Mater. Sol. Cells 95, 2914–2919 (2011).

[12] M. Kröger, S. Hamwi, J. Meyer, T. Riedl, W. Kowalsky, A. Kahn, Organic Electronics, 10, 932-938 (2009).

[13] K. Bange, Sol. Energy Mater. Sol. Cells 58, 1-131 (1999).

[14] X. W. Lou, H. C. Zeng, Chem. Mater. 14, 4781–4789 (2002).

[15] P. Badica, Cryst. Growth Des. 7, 794-801 (2007).

[16] N. A. Chernova, M. Roppolo, A. C. Dillon, M. S. Whittingham, J. Mater. Chem. 19 2526–2552 (2009).

[17] J. Song, X. Ni, L. Gao, L. Zheng, Chem. Phy. 102, 245–248(2007).

[18] S. S. Mahajan, S. H. Mujawar, P. S. Shinde, A. I. Inamdar, P. S. Patil, Int. J. Electrochem. Sci. 3, 953-960 (2008).

[19] C. Raj, A. C. Bose, J. Alloys Compd. 509, 8105-8110 (2011).

[20] L. P. M. Cai, X. R. Zheng, NanoLett. 11, 872–877 (2011).

[21] B. B. Wang, K. Zhu, J. Feng, J. Y . Wu, R. W. Shao, K. Zheng, Q. J. Cheng, Journal of Alloys and Compounds, 661, 66-71 (2016)

[22] D. Y. Park, Y. K. Sun, S. T. Myung, Journal of Power Sources, 280, 1-4 (2015).

[23] C. A. Ellefson, O. Marin-Flores, S. Ha, M. G. Norton, J. Mater. Sci. 47, 2057-2071 (2012).

[24] J. Song, X. Ni, D. Zhang, H. Zheng, Solid State Sci. 8, 1164-1167 (2006).

[25] K. V. Özdokur, A. Y. Tatlı, B. Yılmaz, S. Koçak, F. N. Ertaş, Int. J. of Hydrogen Energy, 41, 5927-5933 (2016).

[26] A. Kumar and G. Pandey, Chemical Science Transactions 2017, 6(3), 385-392, DOI:10.7598/cst2017.1378

[27] M. Karthikeyan, S. Um, Thin Solid Films, 606, 63-73 (2016).

[28] A. Kumar, G. Pandey, *Desalination and Water Treatment,* 71 (2017) 406–419, doi: 10.5004/dwt.2017.20541

[29] R. Yuksel, S. Coskun, H. E. Unalan, Electrochimica Acta, 193, 39-44 (2016).

[30] A. Kumar, G. Pandey, Chem Sci J 8: (2017) 164. doi: 10.4172/2150-3494.1000164

[31] A. Kumar, D. Kumar, G. Pandey. J. Technological Advances and Scientific Res. 2016; 2(4):166-169, DOI: 10.14260/jtasr/2016/29

[32] Y. Song, Y. Zhao, Z. Huang, J. Zhao, Journal of Alloys and Compounds, 693, 1290-1296 (2017).

[33] A. Kumar, G. Hitkari, M. Gautam, S. Singh, G. Pandey, *Int. Adv. Res. J. in Sci.e, Engi. and Tech.*, *2, 12, 2015, 50-55,* DOI 10.17148/IARJSET.2015.21208

[34] M. Bivour, J. Temmler, H. Steinkemper, M. Hermle, Solar Energy Materials and Solar Cells, 142, 34-41 (2015).

[35] A. Kumar, G. Hitkari, M. Gautam, S. Singh, G. Pandey, Int. Journal Inno. Res. in Sci., Eng. and Tech.,. 4, 12, 2015, 12721-12731, DOI:10.15680/IJIRSET.2015.0412097

[36] A. Kumar, G. Pandey. *American J. of Nano Research and Appli.* Vol. 5, No. 4, 2017, pp. 40-48. doi: 10.11648/j.nano.20170504.11

[37] F. Delalat, M. Ranjbar, H. SalamatiSolar Energy Materials and Solar Cells, 144, 165-172 (2016).

[38] Cibele, P. D. Volanti, A. E. Nogueira, C. A. Zamperini, Materials & Design, 115, 73-81 (2017).

[39] E. C. Vergani, E. Longo, G. Totea, D. Ionita, I. Demetrescu, Journal of Bionic Engineering, 12, 583-591 (2015).

[40] S. Shafaei, D. V. Opdenbosch, T. Fey, M. Koch, T Kraus, J. P. Guggenbichler, C. Zollfrank, Materials Science and Engineering: C, 58, 1064-1070 (2016).